Self-Assembly of Two-Dimensional Nanosheets Induced by Interfacial Polyionic Complexation

Jianli Zou and Franklin Kim*

Institute for Integrated Cell-Material Sciences (WPI-iCeMS), Kyoto University, Kyoto 606-8501, Japan

ABSTRACT Significant progress has been made during the past decade in preparing nanosheets from a wide range of materials, which are actively pursued for various applications such as energy storage, catalysis, sensing, and membranes. One of the next critical challenges is developing a robust and versatile assembly method which allows construction of the nanosheets into functional structures tailored for each specific purpose. An interesting characteristic of nanosheets is that they often behave as charged macromolecules and thus can readily interact with an oppositely charged polyelectrolyte to form a stable complex. In this report, we demonstrate how such a complexation process could be utilized for directing the self-assembly of nanosheets. By confining the nanosheet–polyelectrolyte complexation at air–liquid or liquid–liquid interfaces, the nanosheets are successfully assembled into various mesoscale architectures including fibers, capsules, and films. Furthermore, incorporation of additional components such as nanoparticles or small molecules can be easily achieved for further tailoring of material properties. This novel assembly method opens a pathway to many useful nanosheet superstructures and may be further extended to other types of nanomaterials in general.

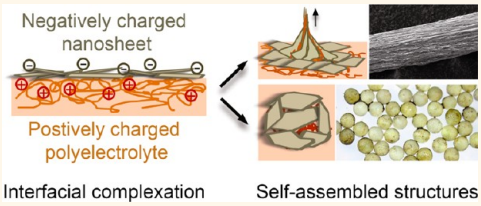

KEYWORDS: nanosheet · self-assembly · interfacial assembly · polyelectrolyte complexation · graphene oxide

Recent advances in delamination methods have enabled easy access to two-dimensional (2D) nanosheets from numerous layered materials, including graphene,[1,2] clay,[3,4] metal oxides,[5,6] and transition metal dichalcogenides (TMDs).[7,8] At the same time, several wet-chemical methods have also been developed for creating various metal[9,10] and metal oxide nanosheets.[11,12] With high surface area and unique properties that differ from its bulk counterparts, these nanosheets are actively pursued for practical applications including membranes,[13,14] electronics,[2,15] energy storage,[5,7,16] sensors,[17] and catalysis.[6,10–12,18,19] However, to fully realize such potential usages, a major challenge remains in developing assembly techniques to construct the nanosheets into well-controlled functional architectures tailored for each specific purpose. An ideal protocol should have flexibility to produce a wide range of structures, be applicable to different types of nanosheets in general, and allow tuning of material properties in a simple way. While several strategies have been reported up to this point such as *in situ* assembly,[20] aerosol processing,[21] and Langmuir–Blodgettry,[14,22,23] their applications are yet somewhat limited.

One method of particular interest is layer-by-layer (LBL) assembly, which typically involves sequential deposition of the nanosheets onto a template along with an oppositely charged polymer, resulting in multilayer structures stabilized by electrostatic interactions. Due to its simplicity and versatility, a wide range of nanosheet–polymer composites have been prepared and tested using this technique.[19,24–29] It is interesting to note that LBL assembly originally evolved from studies on "polyelectrolyte complexation", a term used to describe the formation of a stable macromolecular complex when polyelectrolytes of opposite charges are mixed together. This phenomenon has long been of interest to researchers since a wide range of polymer composites with tunable materials properties could be obtained in a very simple manner.[30,31] More importantly, significant progress has been recently made in confining such complexation to liquid–liquid or liquid–air interfaces, providing further control of the final assembled architecture. Through such interfacial assembly, various

* Address correspondence to fkim@icems.kyoto-u.ac.jp.

Received for review August 9, 2012 and accepted November 7, 2012.

Published online November 07, 2012
10.1021/nn303608g

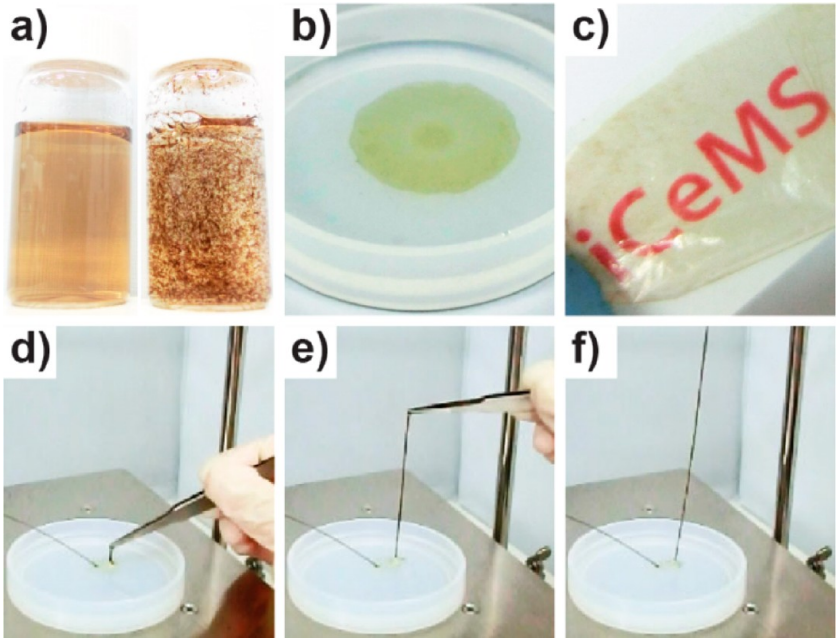

Figure 1. Polyionic complexation between graphene oxide (GO), a negatively charged nanosheet, and chitosan, a positively charged polyelectrolyte. (a) When chitosan is mixed into a GO suspension (left), flocculation occurs immediately (right). (b,c) This complexation can be induced on an air−liquid interface by spreading GO suspension dropwise to the surface of a chitosan solution, resulting in formation of a stable thin film (b), which can later be dried as a free-standing transparent sheet (c). (d−f) Wet film can also be drawn as a fiber by grabbing with a tweezer and gently pulling it up. By replenishing GO using a syringe pump, it is possible to continuously draw long fibers.

polymeric structure including films,[32] fibers,[33,34] capsules,[35] and zipper brushes[36] have been obtained, which have been actively pursued notably for biological applications such as cell culture scaffolds and drug delivery systems.

An interesting characteristic of nanosheets is that they often act as charge-bearing macromolecules and, therefore, readily interact with charged polymers.[4,15,37,38] Given such fact, there is a strong possibility that the complexation of nanosheets with polyelectrolytes may also induce similar self-assembly behaviors which have been observed from the polyelectrolyte−polyelectrolyte systems. Aside from LBL assembly, there have been very limited studies on how the interaction of nanosheets with polyelectrolytes may be utilized to direct their self-assembly. Considering the rich phenomena observed from polyelectrolyte complexation, we believe that there are vast uncharted areas which could be further exploited. Therefore, in this report, we examine the complexation between nanosheets and polyelectrolytes at different types of interfaces and the various assembled superstructures derived from it.

RESULTS AND DISCUSSION

We start the discussion using graphene oxide (GO), which has been one of the most studied nanosheets during the past several years, mostly as a precursor for graphene-based materials. GO serves as an ideal model 2D material since a bulk amount of ultrathin sheets can be obtained using relatively simple reactions. The sheets are flexible and have negative surface charges due to ionization of carboxylic acid and hydroxyl groups; therefore, it has often been considered as a charged macromolecule.[14,39−41] We tested the interaction of GO with chitosan, a widely used cationic biopolymer for agricultural and medical applications. A modified Hummers method was used to prepare GO.[42] SEM and AFM images show that the product largely consists of nanosheets with lateral size in the range of few micrometers to tens of micrometers and thickness less than a nanometer (Figure S1 in Supporting Information). When a small amount of chitosan was mixed into a stable suspension of GO, immediate flocculation was observed, clearly demonstrating strong interactions between the nanosheet and polymer (Figure 1a).

To investigate the assembly of GO and chitosan at an air−liquid interface, a Langmuir−Blodgett (LB) type of setup was utilized. First, chitosan solution (0.5 wt % in 0.5 wt % acetic acid) was prepared as an underlying subphase. We then gently applied GO suspension (10 mg mL^{-1} in 9:1 DMF/water mixture) dropwise onto the chitosan surface so that it spread as a thin film, as shown in Figure 1b. The formed film was strong enough to be easily manipulated with a tweezer and could even be dried up as a free-standing transparent sheet (Figure 1c). SEM images of the dried film show that the GO sheets are mostly stacked in a layered fashion, with a thickness of few hundred nanometers (Figure S2). Similar experiments were conducted on an acetic acid

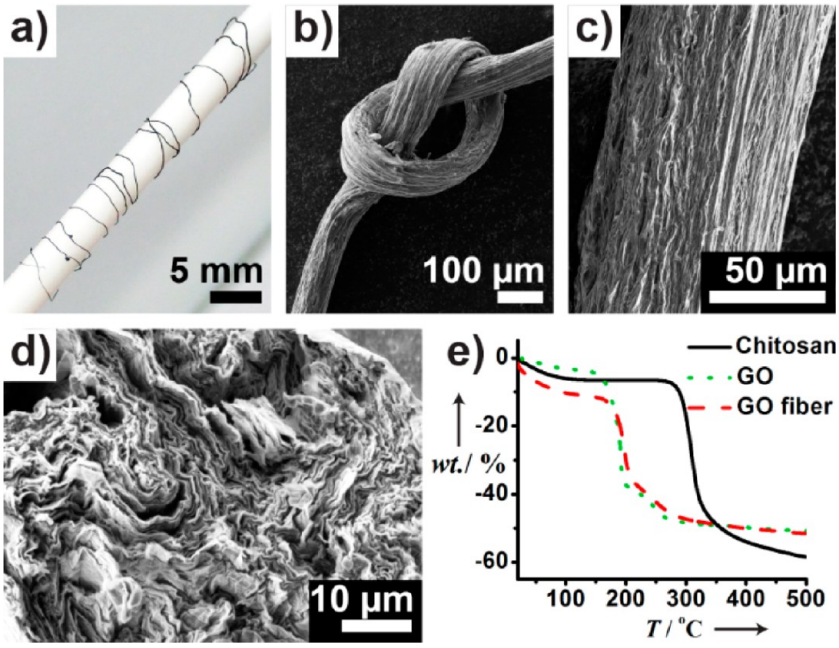

Figure 2. GO fibers after drying in ambient conditions. (a) Final fibers are flexible and strong enough to be easily wound around a thin rod or (b) tied as a knot. Scanning electron microscopy (SEM) images on the (c) side and (d) cross section of the fiber show that the GO sheets are stacked and heavily crumpled but also mostly aligned along the longitudinal direction. (e) Content of GO in the fiber is above 90%, as determined by thermogravimetric analysis (TGA).

solution (0.5 wt %) in the absence of chitosan and also on a solution of poly(acrylic acid) (PAA, 10 wt % in water), which is a negatively charged polymer. In both cases, the GO suspension spreads on the interface but does not form a stable film. This demonstrates that the electrostatic interaction between GO and chitosan is strongly contributing to the mechanical stability of the film structure.

Interestingly, the wet film on chitosan surface could also be drawn as a fiber by grabbing the film with a pair of tweezers and slowly pulling it upward (Figure 1d–f). By constantly adding fresh GO onto the surface using a syringe pump, the removed film can be immediately replenished, allowing continuous drawing of long fibers. We are able to routinely draw fibers over several tens of centimeters with this simple manual procedure, but when coupled with automated roll-up apparatuses used in wet-spinning, it should be possible to achieve even longer lengths. Formation of viscous droplet beads is observed along the GO fibers at relatively faster drawing rates (Figure S3). Such phenomena have also been noticed during wet-spinning of fibers from polyelectrolyte–polyelectrolyte complexation,[33,43] suggesting that a similar self-assembly process is driving the generation of fibers.

When the as-prepared GO fiber is hang-dried in ambient conditions, it shrinks significantly in both diameter and length. However, the fiber length can be adjusted by fixing the free end to another surface before drying. The final fiber is flexible and strong enough such that it can be easily wound around a thin rod or tied as a knot by hand (Figure 2a,b). SEM images show that the GO sheets are highly crumpled and stacked in the interior but are generally aligned along the length (Figure 2c,d), which suggests that the layered structure of GO film is partially retained during the wet-drawing process. The fiber is initially nonconductive, indicating that GO remains oxidized; however, exposure to hydrazine vapor restores conductivity while preserving the fiber structure. Through thermogravimetric analysis (TGA), we determined that the fibers consist mostly of GO (>90%, Figure 2e). The low content of chitosan was unexpected considering that it serves as a critical component for the initial GO film formation and implies that strong interlayer attraction between the nanosheets may also be playing an important role in keeping the structure intact along with the electrostatic interaction of GO and chitosan.

Such self-assembly should occur not only at liquid–air interfaces but also at liquid–liquid interfaces. As a way to demonstrate this, we applied chitosan solution (2 wt % in 2 wt % acetic acid, ~12 μL) dropwise to a GO suspension (10 mg mL^{-1} in 9:1 DMF/water mixture) using a micropipet. Under this condition, the chitosan droplets sink into the suspension and form stable bead-like structures. Interestingly, the droplets could preserve its spherical shape even after the surrounding GO suspension was drained and were soft but strong enough to allow pinching and manipulation with a pair of tweezers (Figure 3a). When left under ambient conditions, the diameter of the droplets decreased from 2.6 ± 0.1 mm to 0.64 ± 0.06 mm, which suggests evaporation of the encapsulated solvent (Figure 3b,c). SEM images of the final dried structure

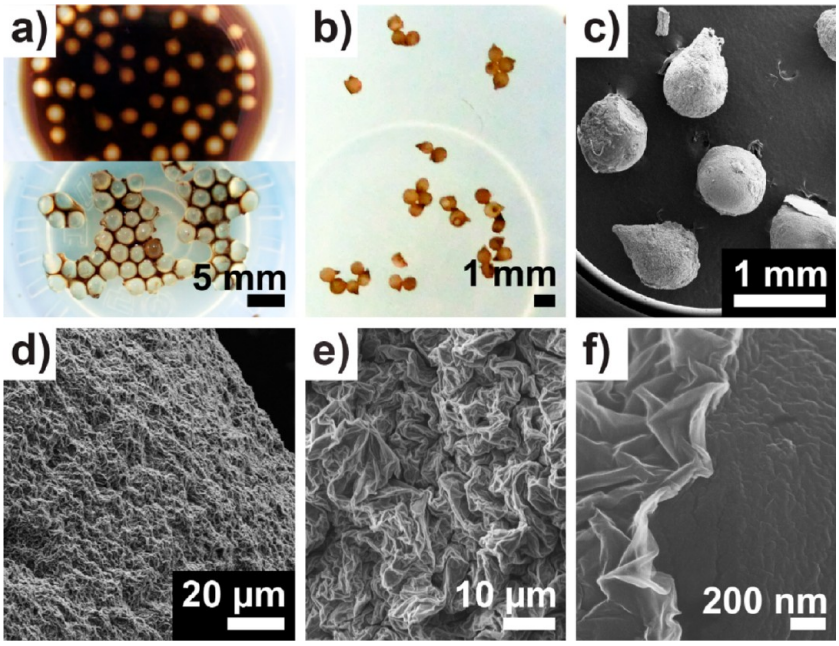

Figure 3. Preparation of capsule structures. (a) When chitosan solution is added dropwise to GO suspension, the droplets sink but maintain a bead-like structure (top), which can stay stable even after the surrounding suspension is removed (bottom). (b,c) When dried in ambient conditions, the droplets shrink in size but preserve their spherical shape. SEM on the (d,e) outer surface and (f) cross section of the dried structure suggest that complexation of GO and chitosan occurs on the liquid−liquid interface, resulting in a layer with a thickness of several tens of nanometers that encapsulates and stabilizes the chitosan solution droplet.

show a highly crumpled layer with a thickness of several tens of nanometers on the outer wall but a relatively smooth and continuous material filling the interior (Figure 3d−f). In addition, TGA result shows that a majority of the structure (~71%) is composed of chitosan (Figure S4). Such observations suggest that, as the chitosan droplet is immersed in GO suspension, complexation of the nanosheets and chitosan occurs on the liquid−liquid interface, resulting in capsule-like structure with a GO layer encapsulating the solution of free-standing chitosan. Crumpling of the capsule wall is most likely due to shrinkage of the whole structure while drying. Even in the absence of GO, when chitosan solution is applied to DMF, the droplets remain stable in the solvent rather than dissolving; however, such droplets readily collapse once the surrounding DMF is removed. This demonstrates that the complexation of GO and chitosan is playing a crucial role on keeping the capsule structure intact. It is intriguing that such a thin layer is able to successfully stabilize the significantly larger droplet. On the basis of our observations from the formation of film and fiber structures, we attribute the mechanical strength to a combined effect of electrostatic interactions of GO and chitosan, along with interlayer interaction between the GO nanosheets.

Up to this point, we have explored how the complexation of GO nanosheets with chitosan can lead to various self-assembled structures. Another strong advantage of this technique is that integration of other components can be easily achieved for additional functionality. For example, to create GO fibers with magnetic properties, we simply prepared a mixed suspension of GO and Fe_3O_4 nanoparticles (average diameter = 19.2 nm) and used it to draw fibers. The obtained fiber does not show much visible difference to that from a pure GO suspension; however, SEM confirms that a large amount of nanoparticles is attached to or embedded within the sheets (Figure 4a). The maximum loading capacity of nanoparticles to GO film we achieved was 1:8 Fe_3O_4/GO in mass (11 wt %). With further increased content of Fe_3O_4 nanoparticles, the film becomes less stable and eventually no longer manipulable with tweezers. In a similar fashion, it is also possible to incorporate Fe_3O_4 nanoparticles into GO capsules by just blending the nanoparticles into chitosan solution before adding dropwise to the GO suspension. The formed beads are much darker in color (Figure 4c) compared to those prepared by pure chitosan solution (Figure 3a), showing that the particles are successfully loaded. Both fibers and capsules are readily attracted to magnetic fields as expected (Figure 4b,d). Other materials such as gold nanorods and water-soluble dye molecules were also loaded to the GO structures without any difficulties (Figures S5 and S6), displaying a wide opportunity for tailoring material properties.

While we have used GO as a model system, in principle, this self-assembly should occur with any type of nanosheets that can interact with a polyelectrolyte.

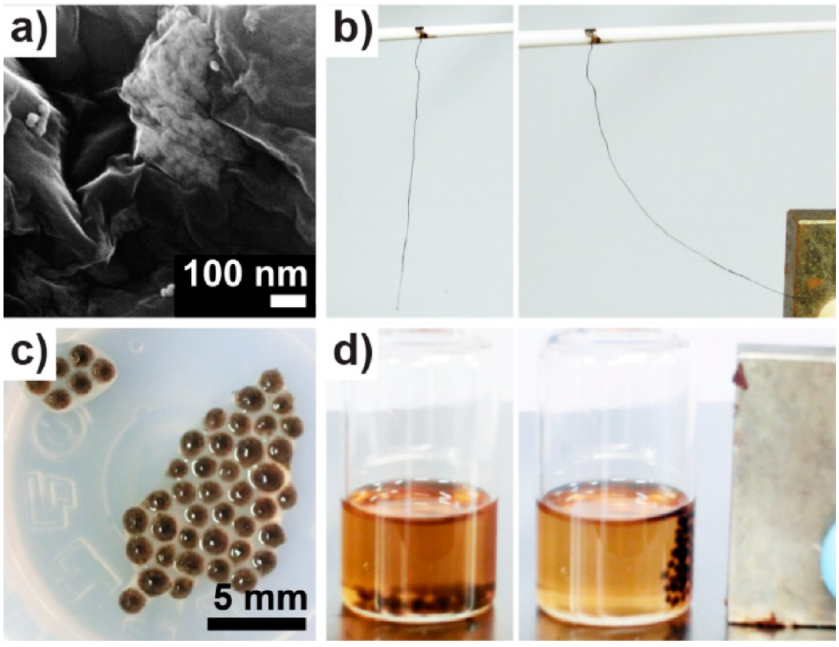

Figure 4. Integration of additional components to the GO structures. (a,b) GO fibers with magnetic properties can be prepared by premixing Fe_3O_4 nanoparticles into a GO suspension and drawing fibers from it as shown in Figure 1. SEM image (a) confirms that the nanoparticles are attached to or embedded within GO sheets. (c,d) Similarly, it is possible to incorporate Fe_3O_4 nanoparticles into GO capsules by using a mixed suspension of chitosan/nanoparticles and following the procedure in Figure 3. The resulting beads are dark in color (c), indicating successful loading of Fe_3O_4 nanoparticles. Both fibers and capsules show strong magnetic responses (b,d).

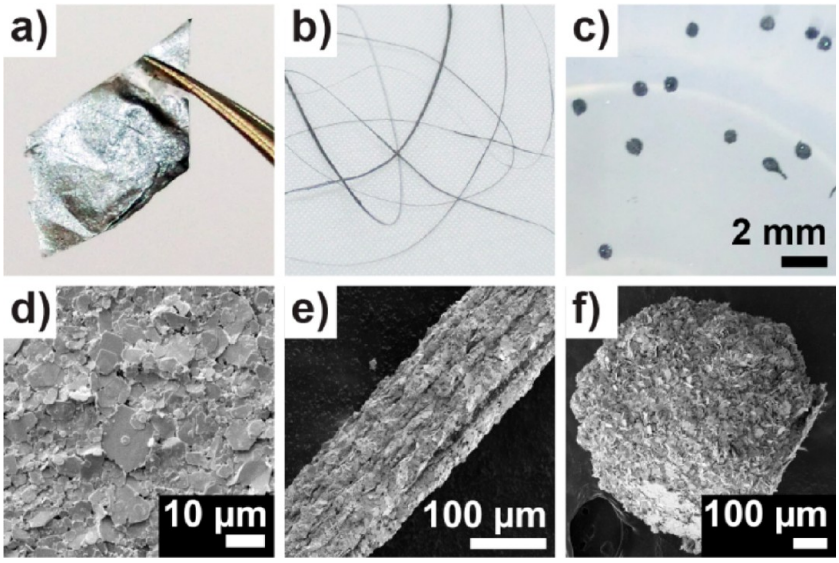

Figure 5. Interfacial assembly with different nanosheets. Despite differences in size and thickness compared to GO, WS_2 nanosheets can readily be constructed into film (a,d), fiber (b,e), and capsule (c,f) structures by using similar experimental procedures described in Figures 1−3. Such self-assembly behavior has also been demonstrated with MoS_2 nanosheets (Supporting Information, Figure S10).

To demonstrate this, we tested WS_2 nanosheets prepared by a sonication-assisted exfoliation method reported by Coleman *et al.*[7] The sheets are negatively charged and have sizes spanning from a few to tens of micrometers (Figure S7), which is comparable to GO. However, the WS_2 nanosheets generally maintain a flat plate-like conformation rather than crumpling, suggesting that they are significantly more rigid than GO. Even with such a difference, immediate flocculation was observed when chitosan was added to a stable suspension of WS_2 nanosheets (Figure S8). In addition, by following similar procedures conducted with GO, we could easily replicate the formation of films, fibers, and capsules, including the incorporation of Fe_3O_4 nanoparticles (Figure 5 and Figure S9). Experiments with MoS_2 nanosheets also yielded comparable

results despite having much smaller sheet sizes in the submicrometer ranges (Figure S10), suggesting that this assembly method could potentially be extended to other nanoparticles such as spheres, rods/wires, and platelets.

CONCLUSION

In conclusion, we have demonstrated that the assembly of 2D nanosheets can be directed in a simple yet effective fashion through interfacial complexation with polyelectrolytes, leading to a variety of architectures including films, fibers, and capsules. Additional components such as nanoparticles and small molecules could also be easily integrated to the structure for further tailoring of material properties. This robust and versatile assembly method opens a pathway to many exciting superstructures of 2D nanosheets. Furthermore, we envision that our discovery will ultimately be applicable to all other types of nanomaterials in general.

EXPERIMENTAL METHODS

Preparation of Graphene Oxide. Graphene oxide (GO) was synthesized using a modified Hummers method reported earlier.[42] In brief, concentrated H_2SO_4 (75 mL) was heated to 80 °C in a 500 mL round-bottom flask. $K_2S_2O_8$ (15 g) and P_2O_5 (15 g) were added to the acid and stirred until fully dissolved. Graphite powder (20 g, Bay Carbon Inc. SP-1 grade) was added to the solution and kept at 80 °C for 4.5 h. The mixture was then cooled, diluted with 1.5 L of deionized (DI) water, and filtered using filter papers (Whatman, grade no. 3). The collected product was further rinsed with DI water (6 times, 1 L each) and dried in air. The powder was then transferred into a 2 L Erlenmeyer flask with concentrated H_2SO_4 (750 mL) and cooled to 5 °C using an ice bath. $KMnO_4$ (100 g) was slowly added to the mixture while stirring. The flask was then transferred to a 35 °C water bath and left for 2 h, and then transferred back into an ice bath. DI water (1 L) was slowly added to the flask while stirring, taking great caution to keep the temperature below 20 °C. The suspension was left for 2 h and diluted with DI water to a total volume of 4 L. Then, 80 mL of a 30% H_2O_2 solution was slowly added to the flask while stirring, forming orange precipitates. The product was filtered using a PTFE membrane (Millipore, Omnipore membrane, 5.0 μm pores), rinsed with 3.4% HCl solution (1 L at a time, up to a total of 6 L), collected, and dried in a desiccator with P_2O_5 as drying agent. The solid was redispersed in acetone, filtered using a PTFE membrane (Millipore, Fluoropore membrane, 3.0 μm pores), further rinsed with additional acetone (1 L at a time, up to a total of 6 L), and dried in ambient conditions. The final product, which is oxidized graphite, was exfoliated into GO by sonicating in solvents such as DMF or water.

Preparation of WS_2 and MoS_2 Nanosheets. WS_2 and MoS_2 nanosheets were prepared using a procedure reported by Coleman *et al.*[7] Briefly, WS_2 and MoS_2 powders (Aldrich) were each sonicated in *N*-methyl formamide (NMP, 0.5 mg mL^{-1}) for 2 h. The exfoliated sheets were purified three times by centrifuging and redispersing in DMF. The final product was kept in DMF until used for further experiments.

Preparation of Fe_3O_4 Nanoparticles. Fe_3O_4 nanoparticles were prepared according to a procedure described by Park *et al.*[44] Surfaces of the Fe_3O_4 nanoparticles were subsequently modified with COOH-carrying silane coupling agent (*n*-(trimethoxysilylpropyl)ethylene diamine triacetic acid) according to the method reported by De Palma *et al.*[45]

Fabrication of GO Film and Fiber. GO suspension (10 mg mL^{-1} in 9:1 DMF/water mixture) was gently applied using a glass pipet onto the surface of a chitosan solution (Sigma, high viscosity, 0.5 wt % in 0.5 wt % acetic acid, pH 4.5) contained in a perfluoroalkoxy (PFA) Petri dish. The GO spreads and forms a thin film on the interface, which can be collected as a free-standing sheet by draining the underlying chitosan solution and drying it under ambient conditions.

For GO fiber preparation, a syringe pump was used to deliver GO suspension onto a chitosan solution surface at the rate of 0.05 mL min^{-1}. The film formed on the surface was picked up using a pair of tweezers and carefully pulled upward. The pulling speed was adjusted to match the formation of fresh film by the continuous addition of GO suspension. The fiber was later hung on a glass or PTFE rod and dried under ambient conditions.

Reduction of GO fiber was done by placing it in an autoclave with a small amount of hydrazine and keeping at 80 °C for overnight.

Fabrication of the GO Capsule. Chitosan solution (2 wt % in 2 wt % acetic acid, pH 4.5) was added dropwise using a micropipet to a GO suspension (10 mg mL^{-1} in 9:1 DMF/water mixture solvent) in a PTFE vessel. The volume of chitosan solution was fixed at ~12 μL for this study. The applied droplets sink into the GO suspension and form stable bead-like structures. The vessel was left on a shaker overnight. To collect the formed capsules, the GO suspension was simply removed using a pipet. Loading the capsules with other components such as small molecules or nanoparticles was achieved by blending the material of interest into the chitosan solution before application to the GO suspension. For the sample shown in Figure 4c, a ratio of chitosan/Fe_3O_4 = 18:1 (in weight) was used.

Characterization. Scanning electron microscope (SEM) images were taken with a JEOL JSM-7001 F4 microscope, using an acceleration voltage in the range of 2 to 15.0 kV. The samples were generally drop-cast onto a piece of silicon wafer or fixed on conductive copper tape. To minimize charging effects, a less than 5 nm layer of osmium was applied to nonconductive samples prior to imaging.

AFM was performed with an Agilent Technologies 5500AFM system, operated in AAC mode. Images were recorded under ambient conditions at a scan rate of 1 Hz. Silicon cantilevers with nominal spring constant in the range of 2−3 N/m and resonance frequency of 73−82 kHz (Olympus, AC240) were used.

Thermogravimetric analysis was done using a Thermo plus EVO II system. Prior to measurement, all samples were dried in an oven at 80 °C for 24 h and then stored in a vacuum chamber until tested. GO, chitosan, GO fiber, and capsule were each examined under N_2 atmosphere from 25 to 500 °C, at a heating rate of 10 °C min^{-1}. Percentage of chitosan within the GO fiber and capsule structures was determined by comparing the mass loss from 25 to 500 °C.

Conflict of Interest: The authors declare no competing financial interest.

Acknowledgment. This work was supported by the Institute for Integrated Cell-Material Sciences (iCeMS). iCeMS is supported by the World Premier International Research Center Initiative (WPI), MEXT, Japan. We are grateful to N. Morone at iCeMS and the Center for Meso-Bio Single-Molecule Imaging (CeMI) for assistance in electron microscopy. We also thank S. Yamamoto at iCeMS for generously providing Fe_3O_4 nanoparticles.

Supporting Information Available: Supplementary figures including SEM image of GO film, digital camera image of GO fiber formation, SEM image of GO fiber loaded with gold nanorod, image of GO capsules loaded with green dye molecules, zeta-potential distribution of WS_2 and MoS_2 nanosheets, self-assembled structures of WS_2 and MoS_2 nanosheets prepared through complexation with chitosan. This material is available free of charge *via* the Internet at http://pubs.acs.org.

REFERENCES AND NOTES

1. Stankovich, S.; Dikin, D. A.; Piner, R. D.; Kohlhaas, K. A.; Kleinhammes, A.; Jia, Y.; Wu, Y.; Nguyen, S. T.; Ruoff, R. S. Synthesis of Graphene-Based Nanosheets *via* Chemical Reduction of Exfoliated Graphite Oxide. *Carbon* **2007**, *45*, 1558–1565.
2. Hernandez, Y.; Nicolosi, V.; Lotya, M.; Blighe, F. M.; Sun, Z.; De, S.; McGovern, I. T.; Holland, B.; Byrne, M.; Gun'Ko, Y. K.; *et al.* High-Yield Production of Graphene by Liquid-Phase Exfoliation of Graphite. *Nat. Nanotechnol.* **2008**, *3*, 563–568.
3. Nadeau, P. H.; Wilson, M. J.; Mchardy, W. J.; Tait, J. M. Interstratified Clays as Fundamental Particles. *Science* **1984**, *225*, 923–925.
4. Sasaki, T.; Watanabe, M.; Hashizume, H.; Yamada, H.; Nakazawa, H. Macromolecule-like Aspects for a Colloidal Suspension of an Exfoliated Titanate. Pairwise Association of Nanosheets and Dynamic Reassembling Process Initiated from It. *J. Am. Chem. Soc.* **1996**, *118*, 8329–8335.
5. Sugimoto, W.; Iwata, H.; Yasunaga, Y.; Murakami, Y.; Takasu, Y. Preparation of Ruthenic Acid Nanosheets and Utilization of Its Interlayer Surface for Electrochemical Energy Storage. *Angew. Chem., Int. Ed.* **2003**, *42*, 4092–4096.
6. Takagaki, A.; Sugisawa, M.; Lu, D.; Kondo, J. N.; Hara, M.; Domen, K.; Hayashi, S. Exfoliated Nanosheets as a New Strong Solid Acid Catalyst. *J. Am. Chem. Soc.* **2003**, *125*, 5479–5485.
7. Coleman, J. N.; Lotya, M.; O'Neill, A.; Bergin, S. D.; King, P. J.; Khan, U.; Young, K.; Gaucher, A.; De, S.; Smith, R. J.; *et al.* Two-Dimensional Nanosheets Produced by Liquid Exfoliation of Layered Materials. *Science* **2011**, *331*, 568–571.
8. Ramakrishna Matte, H. S. S.; Gomathi, A.; Manna, A. K.; Late, D. J.; Datta, R.; Pati, S. K.; Rao, C. N. R. MoS_2 and WS_2 Analogues of Graphene. *Angew. Chem., Int. Ed.* **2010**, *49*, 4059–4062.
9. Kim, J. U.; Cha, S. H.; Shin, K.; Jho, J. Y.; Lee, J. C. Preparation of Gold Nanowires and Nanosheets in Bulk Block Copolymer Phases under Mild Conditions. *Adv. Mater.* **2004**, *16*, 459–464.
10. Huang, X.; Tang, S.; Mu, X.; Dai, Y.; Chen, G.; Zhou, Z.; Ruan, F.; Yang, Z.; Zheng, N. Freestanding Palladium Nanosheets with Plasmonic and Catalytic Properties. *Nat. Nanotechnol.* **2011**, *6*, 28–32.
11. Han, X.; Kuang, Q.; Jin, M.; Xie, Z.; Zheng, L. Synthesis of Titania Nanosheets with a High Percentage of Exposed (001) Facets and Related Photocatalytic Properties. *J. Am. Chem. Soc.* **2009**, *131*, 3152–3153.
12. Kuo, C.-L.; Kuo, T.-J.; Huang, M. H. Hydrothermal Synthesis of ZnO Microspheres and Hexagonal Microrods with Sheetlike and Platelike Nanostructures. *J. Phys. Chem. B* **2005**, *109*, 20115–20121.
13. Nikoobakht, B.; Li, X. Two-Dimensional Nanomembranes: Can They Outperform Lower Dimensional Nanocrystals? *ACS Nano* **2012**, *6*, 1883–1887.
14. Kulkarni, D. D.; Choi, I.; Singamaneni, S. S.; Tsukruk, V. V. Graphene Oxide–Polyelectrolyte Nanomembranes. *ACS Nano* **2010**, *4*, 4667–4676.
15. Osada, M.; Sasaki, T. Two-Dimensional Dielectric Nanosheets: Novel Nanoelectronics from Nanocrystal Building Blocks. *Adv. Mater.* **2012**, *24*, 210–228.
16. Yoo, E.; Kim, J.; Hosono, E.; Zhou, H.-s.; Kudo, T.; Honma, I. Large Reversible Li Storage of Graphene Nanosheet Families for Use in Rechargeable Lithium Ion Batteries. *Nano Lett.* **2008**, *8*, 2277–2282.
17. Wang, Y.; Li, Z.; Hu, D.; Lin, C.-T.; Li, J.; Lin, Y. Aptamer/Graphene Oxide Nanocomplex for *In Situ* Molecular Probing in Living Cells. *J. Am. Chem. Soc.* **2010**, *132*, 9274–9276.
18. Gunjakar, J. L.; Kim, T. W.; Kim, H. N.; Kim, I. Y.; Hwang, S. J. Mesoporous Layer-by-Layer Ordered Nanohybrids of Layered Double Hydroxide and Layered Metal Oxide: Highly Active Visible Light Photocatalysts with Improved Chemical Stability. *J. Am. Chem. Soc.* **2011**, *133*, 14998–15007.
19. Izawa, K.; Yamada, T.; Unal, U.; Ida, S.; Altuntasoglu, O.; Koinuma, M.; Matsumoto, Y. Photoelectrochemical Oxidation of Methanol on Oxide Nanosheets. *J. Phys. Chem. B* **2006**, *110*, 4645–4650.
20. Mo, M.; Yu, J. C.; Zhang, L.; Li, S. K. A. Self-Assembly of ZnO Nanorods and Nanosheets into Hollow Microhemispheres and Microspheres. *Adv. Mater.* **2005**, *17*, 756–760.
21. Chen, Y.; Guo, F.; Jachak, A.; Kim, S. P.; Datta, D.; Liu, J.; Kulaots, I.; Vaslet, C.; Jang, H. D.; Huang, J.; *et al.* Aerosol Synthesis of Cargo-Filled Graphene Nanosacks. *Nano Lett.* **2012**, *12*, 1996–2002.
22. Muramatsu, M.; Akatsuka, K.; Ebina, Y.; Wang, K.; Sasaki, T.; Ishida, T.; Miyake, K.; Haga, M.-a. Fabrication of Densely Packed Titania Nanosheet Films on Solid Surface by Use of Langmuir–Blodgett Deposition Method without Amphiphilic Additives. *Langmuir* **2005**, *21*, 6590–6595.
23. Cote, L. J.; Kim, F.; Huang, J. Langmuir–Blodgett Assembly of Graphite Oxide Single Layers. *J. Am. Chem. Soc.* **2008**, *131*, 1043–1049.
24. Keller, S. W.; Kim, H.-N.; Mallouk, T. E. Layer-by-Layer Assembly of Intercalation Compounds and Heterostructures on Surfaces: Toward Molecular "Beaker" Epitaxy. *J. Am. Chem. Soc.* **1994**, *116*, 8817–8818.
25. Kleinfeld, E. R.; Ferguson, G. S. Stepwise Formation of Multilayered Nanostructural Films from Macromolecular Precursors. *Science* **1994**, *265*, 370–373.
26. Podsiadlo, P.; Michel, M.; Lee, J.; Verploegen, E.; Wong Shi Kam, N.; Ball, V.; Lee, J.; Qi, Y.; Hart, A. J.; Hammond, P. T.; *et al.* Exponential Growth of LbL Films with Incorporated Inorganic Sheets. *Nano Lett.* **2008**, *8*, 1762–1770.
27. Srivastava, S.; Kotov, N. A. Composite Layer-by-Layer (LbL) Assembly with Inorganic Nanoparticles and Nanowires. *Acc. Chem. Res.* **2008**, *41*, 1831–1841.
28. Zhou, Y.; Ma, R. Z.; Ebina, Y.; Takada, K.; Sasaki, T. Multilayer Hybrid Films of Titania Semiconductor Nanosheet and Silver Metal Fabricated *via* Layer-by-Layer Self-Assembly and Subsequent UV Irradiation. *Chem. Mater.* **2006**, *18*, 1235–1239.
29. Zhao, X.; Zhang, Q.; Hao, Y.; Li, Y.; Fang, Y.; Chen, D. Alternate Multilayer Films of Poly(vinyl alcohol) and Exfoliated Graphene Oxide Fabricated *via* a Facial Layer-by-Layer Assembly. *Macromolecules* **2010**, *43*, 9411–9416.
30. Philipp, B.; Dautzenberg, H.; Linow, K.-J.; Kötz, J.; Dawydoff, W. Polyelectrolyte Complexes—Recent Developments and Open Problems. *Prog. Polym. Sci.* **1989**, *14*, 91–172.
31. Gucht, J. v. d.; Spruijt, E.; Lemmers, M.; Cohen Stuart, M. A. Polyelectrolyte Complexes: Bulk Phases and Colloidal Systems. *J. Colloid Interface Sci.* **2011**, *361*, 407–422.
32. Michaels, A. S.; Miekka, R. G. Polycation–Polyanion Complexes: Preparation and Properties of Poly-(vinylbenzyl trimethylammonium) Poly-(styrenesulfonate). *J. Phys. Chem.* **1961**, *65*, 1765–1773.
33. Wan, A. C. A.; Leong, M. F.; Toh, J. K. C.; Zheng, Y.; Ying, J. Y. Multicomponent Fibers by Multi-interfacial Polyelectrolyte Complexation. *Adv. Healthcare Mater.* **2012**, *1*, 101–105.
34. Amaike, M.; Senoo, Y.; Yamamoto, H. Sphere, Honeycomb, Regularly Spaced Droplet and Fiber Structures of Polyion Complexes of Chitosan and Gellan. *Macromol. Rapid Commun.* **1998**, *19*, 287–289.
35. Ohkawa, K.; Kitagawa, T.; Yamamoto, H. Preparation and Characterization of Chitosan–Gellan Hybrid Capsules Formed by Self-Assembly at an Aqueous Solution Interface. *Macromol. Mater. Eng.* **2004**, *289*, 33–40.
36. de Vos, W. M.; Kleijn, J. M.; de Keizer, A.; Cohen Stuart, M. A. Ultradense Polymer Brushes by Adsorption. *Angew. Chem., Int. Ed.* **2009**, *48*, 5369–5371.
37. Kang, H.; Huang, G.; Ma, S.; Bai, Y.; Ma, H.; Li, Y.; Yang, X. Coassembly of Inorganic Macromolecule of Exfoliated LDH Nanosheets with Cellulose. *J. Phys. Chem. C* **2009**, *113*, 9157–9163.
38. Skirtach, A. G.; Déjugnat, C.; Braun, D.; Susha, A. S.; Rogach, A. L.; Sukhorukov, G. B. Nanoparticles Distribution Control by Polymers: Aggregates *versus* Nonaggregates. *J. Phys. Chem. C* **2006**, *111*, 555–564.
39. Guo, F.; Kim, F.; Han, T. H.; Shenoy, V. B.; Huang, J.; Hurt, R. H. Hydration-Responsive Folding and Unfolding in Graphene

Oxide Liquid Crystal Phases. *ACS Nano* **2011**, *5*, 8019–8025.
40. Manga, K. K.; Zhou, Y.; Yan, Y.; Loh, K. P. Multilayer Hybrid Films Consisting of Alternating Graphene and Titania Nanosheets with Ultrafast Electron Transfer and Photoconversion Properties. *Adv. Funct. Mater.* **2009**, *19*, 3638–3643.
41. Kim, J.; Cote, L. J.; Kim, F.; Yuan, W.; Shull, K. R.; Huang, J. Graphene Oxide Sheets at Interfaces. *J. Am. Chem. Soc.* **2010**, *132*, 8180–8186.
42. Kim, F.; Luo, J. Y.; Cruz-Silva, R.; Cote, L. J.; Sohn, K.; Huang, J. X. Self-Propagating Domino-like Reactions in Oxidized Graphite. *Adv. Funct. Mater.* **2010**, *20*, 2867–2873.
43. Ohkawa, K.; Takahashi, Y.; Yamamoto, H. Self-Assembling Capsule and Fiber Formations of Polyion Complexes of Chitosan and Poly(α,L-glutamic acid). *Macromol. Rapid Commun.* **2000**, *21*, 223–225.
44. Park, J.; An, K.; Hwang, Y.; Park, J. G.; Noh, H. J.; Kim, J. Y.; Park, J. H.; Hwang, N. M.; Hyeon, T. Ultra-Large-Scale Syntheses of Monodisperse Nanocrystals. *Nat. Mater.* **2004**, *3*, 891–895.
45. De Palma, R.; Peeters, S.; Van Bael, M. J.; Van den Rul, H.; Bonroy, K.; Laureyn, W.; Mullens, J.; Borghs, G.; Maes, G. Silane Ligand Exchange To Make Hydrophobic Superparamagnetic Nanoparticles Water-Dispersible. *Chem. Mater.* **2007**, *19*, 1821–1831.